JOURNAL OF GUIDANCE, CONTROL, AND DYNAMICS
Vol. 29, No. 6, November–December 2006

Quasilinear Parameter-Varying Autopilot Design Using Polynomial Eigenstructure Assignment with Actuator Constraints

L. Bruyere,* A. Tsourdos,* and B. A. White*
Cranfield University, Shrivenham, Swindon SN6 8LA England, United Kingdom

DOI: 10.2514/1.17039

In this paper, eigenstructure assignment is used in a polynomial matrix framework. In particular, such eigenstructure assignment does not impose any particular eigenvalues and the assignment is done in one-single pass over the flight envelope of a nonlinear missile. The eigenspace of the system is manipulated in polynomial matrix form and the closed-loop transfer function is expressed as a coprime factorization. The designer is left to choose the controller structure producing a flexible design approach. The approach enables the design to consider both static and dynamic controllers alike. In this paper, the approach is applied to a quasilinear parameter-varying missile and it is simple, attractive and comparable to other approaches while leading to a closed-loop system independent of the operating point. The approach is thus similar to dynamic inversion with a self-scheduled controller, but without the need to consider zero dynamics. A tail-controlled missile in the cruciform fin configuration is modeled as a second-order quasilinear parameter-varying system. A lateral velocity controller is designed for the nonlinear model of a tactical missile. The actuator dynamics are included and successively, the actuator dimensioning and the actuator dynamics effects are traded off against performance using the matching conditions developed herein.

I. Introduction

THE dynamic performance of aerospace systems such as aircraft, spacecraft, and missiles is highly dependent on the capabilities of the guidance, navigation, and control systems [1–3]. To achieve improved performance in such aerospace systems, it is important that more sophisticated control systems be developed and implemented. Very often actuator dynamics are not considered in many nonlinear missile control systems. Most approaches to nonlinear autopilot design assume that the actuator dynamics are fast enough to be neglected in the design. However, missile actuators are limited in performance due to the restricted power sources carried on board. This, in turn, will limit the final performance achievable in any design [1,2,4,5], unless the actuator dynamics are included in the design.

To address this problem, this paper describes a side-slip velocity autopilot design for a realistic model of a tactical missile and examines the impact of actuator dynamics on the missile controller performance.

The missile autopilot design is based on a polynomial eigenstructure assignment [6,7], which expresses the eigenspace of a system as a polynomial function of the closed-loop eigenvalues. This allows a parametric design of the closed-loop eigenspace. Polynomial eigenstructure assignment has been shown to produce successful designs for VSTOL aircraft [6–8] and unmanned underwater vehicles [9]; capturing various objectives including stability, settling time, damping, the decoupling of channels, actuation dynamics limitation, and robustness to disturbances. A broader class of systems, linear parameter-varying (LPV) systems, can similarly be tackled by designing a parameter-dependent controller with this approach. It should be noted that such a design stays valid only for slow varying parameters, as is true for most of the parametric approaches in the literature. For example, if the first-order tangent system provides "sufficient" information about the underlying nonlinear system, LPV analysis and design can be employed. However, application becomes rather difficult to deploy because the interpolation process may be difficult for most systems.

In this paper, using the polynomial eigenstructure assignment (PEA) approach to compute the symbolic polynomial null spaces overcomes this problem and enables the design of a LPV controller to be facilitated. The PEA approach produces a consistent closed-loop performance over the operating range of the missile dynamics. Unlike nonlinear dynamic inversion techniques, PEA deals with any nonminimum phase zeros in the closed-loop system design and does not require any cancellation to produce a standard feedback form. Because the eigenspace is computed in symbolic form, the eigenstructure can be explored parametrically. This means that the effect of both actuator dynamics and the inclusion or deletion of feedback loops can be investigated. Hence, the presence or lack of a particular sensor and its associated feedback can be assessed, as well as having the ability to trade off closed-loop performance against the speed of response of actuators that can be examined, thus giving additional insight to the designer.

A tail-controlled missile in the cruciform fin configuration [10] is modeled as a second-order quasilinear parameter-varying system (QLPV) and is used in the design. This nonlinear model is obtained from the Taylor linearized model of the horizontal motion by including explicit dependence of the aerodynamic derivatives on the missile incidence as well as the Mach number. Hence, the model is state dependent and also has exogenous dependency. This model is considered in the LPV framework where the polynomial eigenstructure assignment approach stays simple, attractive, and comparable to other dynamic inversion approaches and results in a controller in QLPV form. The missile is a nonminimum phase, as it uses rear control actuators with either first- or second-order actuator dynamics.

The designs are tested on nonlinear simulations to demonstrate the effectiveness of the techniques. The studies show the effect of reducing the bandwidth of the actuators on the overall performance and also look at removing feedback loops that are difficult to measure. This takes the state feedback results and converts the system to output feedback, with a parametric study to show the effect on closed-loop performance.

In many applications, but especially aerospace applications, closed-loop performance criteria can often be interpreted by identifying an appropriate eigenstructure, which captures most

Presented as Paper 6383 at the AIAA GNC/AFM/MST Conference and Exhibit, San Francisco, California, 15–17 August 2005; received 7 April 2005; revision received 7 March 2006; accepted for publication 7 March 2006.

*Department of Aerospace, Power and Sensors.

design criteria such as stability, performance, robustness, sensitivity, decoupling, and actuation dynamics. For many years, eigenstructure assignment has been of interest in the context of linear time-invariant systems and has led to powerful tools both for analysis and design [11,12]. A survey of the eigenstructure assignment [13] presents early research and classical algorithms, describing how accessing the system eigenstructure, by examination of both the eigenvalues and their associated eigenvectors, provides a natural mechanism to shape the closed-loop performance. Specific metrics can be constructed that allow the selection of the eigenstructure to meet design criteria such as closed-loop stability, performance, mode decoupling, and robustness. Additional metrics that take account of actuation dynamics and sensitivity can also be constructed. Another interesting feature of polynomial eigenstructure assignment is that both static and dynamic controllers can be designed to enable tradeoffs between controller complexity and performance to be undertaken.

The polynomial eigenstructure assignment was developed by White [6,7]. The initial motivation was to preserve the eigenstructure assignment approach while retaining the eigenvalue constellation as a design parameter, rather than preassigning the eigenvalues. Thus polynomial eigenstructure assignment does not impose a particular set of eigenvalues at the start of the design, but instead uses polynomial matrix computation to produce an eigenspace parameterized by eigenvalues. Classical eigenstructure assignment approaches usually require a given initial partial eigenstructure to produce a controller design. These approaches can lead to solutions that require large feedback gains and poor controllability properties. They can also lead to sensitive designs, although there exist eigenvalue and eigenvector sensitivity criteria to quantify and reduce this effect. It is usually difficult to select the appropriate eigenstructure, and designers customarily resort to several design iterations before a final eigenstructure is determined. PEA expresses the eigenspace as eigenvalue functions, and hence the selection of the eigenvalue constellation can be used as a design parameter during the design process. The open-loop transfer function is written as a coprime factorization of polynomial matrices [14] and hence captures the case of output feedback with dynamic controllers, while retaining the insight of the state derived eigenstructure. These arguments make polynomial eigenstructure assignment consistent, intuitive, and a bridge between state space and Laplace transform. Successful applications of PEA to VSTOL [6–8] and unmanned underwater vehicles [9] illustrate the design process, using metric that measure stability, settling time, damping, the decoupling of channels, actuation dynamics limitation, as well as robustness to disturbances. Another feature of the approach for application to missile autopilot design is that nonminimum phase systems can be designed without the problems associated with dynamic inversion approaches.

For the missile autopilot design, a controller structure has been chosen to give enough design freedom to produce a stable robust autopilot design for the nonlinear dynamics. This structure is suitable for most aerospace applications but it is stressed that the controller structure is not solely restricted to the one presented in this work. To apply PEA, like most techniques, the system is assumed to be controllable and observable, which is often the case in aerospace applications. The theoretical results are valid for MIMO systems, although in the this paper, PEA is applied to a SISO Horton missile model in quasi-LPV form which includes actuator dynamics.

II. Polynomial Eigenstructure Assignment

Assuming the linear time invariant (LTI) system in Eq. (1),

$$\dot{x} = Ax + Bu \tag{1a}$$

$$y = Cx + Du \tag{1b}$$

the eigenvalue/eigenvector null space equation can be written as a polynomial null space equation as shown in Eq. (2):

$$\begin{bmatrix} (A - sI) & B \end{bmatrix} \begin{bmatrix} Z(s) \\ P(s) \end{bmatrix} = 0 \tag{2}$$

where s represents both the eigenvalue and the Laplace variable. $Z(s)$ and $P(s)$ represent the eigenvector space and its associated control vector space, respectively. In the sequel the eigenvectors and/or eigenspace are referred to by their corresponding polynomial matrices.

The open-loop transfer function $G_y(s)$ can be written as

$$G_y(s) = C(sI - A)^{-1}B + D \tag{3}$$

and hence becomes a function of the eigenspace and its associate space as described in (2). So

$$\begin{aligned} G_y(s) &= CZ(s)P(s)^{-1} + D = [CZ(s) + DP(s)]P(s)^{-1} \\ &= Z_0(s)P(s)^{-1} \end{aligned} \tag{4}$$

where

$$Z_o(s) = [CZ(s) + DP(s)] \tag{5}$$

Using PEA, specifying a particular controller structure enables the designer to change the dynamics of the open-loop system without having to cancel out the zero dynamics. The next section introduces a particular controller structure presenting sufficient flexibility for the purpose of aerospace application under consideration in this paper.

A. Controller Structure

The controller structure [7] choice is driven by considerations of improving stability, performance, tracking, sensitivity, and robustness of the system. The controller structure shown in Fig. 1 gives sufficient flexibility to produce such a design. The outputs of the system are partitioned into controlled outputs y_c, and the inner loop outputs y_i. For the missile, controlled output are incidence, side-slip velocity, or acceleration, whereas the inner loop outputs are body rates from rate gyros. Both are required for good performance and robustness. The controller $K_a(s)$ shapes the tracking response of the closed-loop system to the desired demands, the controller $K_u(s)$ shapes the input to the plant, $K_i(s)$ feedback the extra measurements available y_i and $K_c(s)$ feedback the controlled output y_c shaping consequently its transient response. Altogether gains $K_u(s)$, $K_a(s)$, $K_c(s)$, and $K_i(s)$ compose a dynamic controller. For the case where the order of $K_u(s)$ meets or exceeds the order of the other polynomial matrices $K_a(s)$, $K_c(s)$, and $K_i(s)$, the resulting dynamic controller is proper and thus can be realized.

From the figure, the following system interconnection can be defined, where for clarity dependency in s is dropped:

$$u = K_u^{-1}(K_a e - K_c y_c - K_i y_i) \tag{6a}$$

$$y_c = G_c u \tag{6b}$$

$$y_i = G_i u \tag{6c}$$

$$e = r_1 - y_c \tag{6d}$$

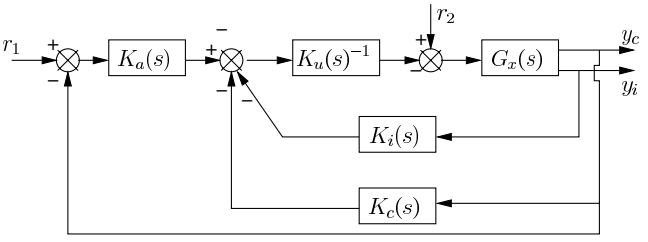

Fig. 1 Controller structure chosen for aerospace applications introducing dynamic gains $K_u(s)$, $K_a(s)$, $K_c(s)$, and $K_i(s)$ with y_c the controlled outputs, and y_i the additional measured outputs.

$$e_u = r_2 - u \tag{6e}$$

where $G_c(s)$ and $G_i(s)$ represent open-loop transfer functions for the controlled and the inner loop outputs, respectively.

The transfer functions for the closed-loop system inputs and outputs are given by

$$\begin{bmatrix} u \\ y_c \end{bmatrix} = \begin{bmatrix} \Delta^{-1}K_u^{-1}K_a & -\Delta^{-1}K_u^{-1}[(K_c+K_a)G_c + K_iG_i] \\ G_c\Delta^{-1}K_u^{-1}K_a & G_c\{I - \Delta^{-1}K_u^{-1}[(K_c+K_a)G_c + K_iG_i]\} \end{bmatrix} \times \begin{bmatrix} r_1 \\ r_2 \end{bmatrix} \tag{7}$$

where $\Delta = \{I + K_u^{-1}[(K_a + K_c)G_c + K_iG_i]\}$ is the transfer function of the open-loop system.

From Eq. (7), four transfer functions can be defined, as follows:

$$T_{ur_1}(s) = \Delta^{-1}K_u^{-1}K_a \tag{8a}$$

$$T_{ur_2}(s) = -\Delta^{-1}K_u^{-1}[(K_c + K_a)G_c + K_iG_i] \tag{8b}$$

$$T_{yr_1}(s) = G_c\Delta^{-1}K_u^{-1}K_a \tag{8c}$$

$$T_{yr_2}(s) = G_c\left\{I - \Delta^{-1}K_u^{-1}[(K_c + K_a)G_c + K_iG_i]\right\} \tag{8d}$$

where $T_{yr_1}(s)$ is the reference input response of the output, $T_{yr_2}(s)$ is its corresponding disturbance response of the outputs, $T_{ur_1}(s)$ is the actuator response to the reference input, and $T_{ur_2}(s)$ is the actuator response to the disturbance input.

As the outputs are partitioned into controlled and other outputs, the transfer functions $T_{yr_1}(s)$ and $T_{yr_2}(s)$ can be split into transfer functions relating to the controlled outputs and the inner loop outputs. Each of them can be written in the form of Eq. (4) and thus lead to two eigenvectors composing $Z_0(s)$, namely, $Z_0^c(s)$ and $Z_0^i(s)$, or

$$Z_0(s) = \begin{bmatrix} Z_0^c(s) \\ Z_0^i(s) \end{bmatrix} \tag{9}$$

These relate to their respective open-loop transfer functions, $G_c(s)$ and $G_i(s)$. In fact, for a controllable and observable system, their coprime factorizations are given by

$$G_c(s) = Z_0^c(s)P(s)^{-1} \tag{10a}$$

$$G_i(s) = Z_0^i(s)P(s)^{-1} \tag{10b}$$

Using Eqs. (10), each transfer function developed in (8) can be expanded using the eigenvector polynomial forms, $Z_0^c(s)$ and $Z_0^i(s)$, and their common polynomial associate polynomial matrix $P(s)$. The reference input response transfer function, $T_{yr_1}(s)$, is then given by

$$\begin{aligned} T_{yr_1}(s) &= Z_0^cP^{-1}\left\{I + K_u^{-1}[(K_a+K_c)Z_0^cP^{-1} + K_iZ_0^iP^{-1}]\right\}^{-1}K_u^{-1}K_a \\ &= Z_0^c\Big[K_uP + (K_a+K_c)Z_0^c + K_iZ_0^i\Big]^{-1}K_a \end{aligned} \tag{11}$$

The remaining transfer functions can also be defined in a similar manner. For example, the actuator response transfer function, $T_{ur_1}(s)$, is given by

$$\begin{aligned} T_{ur_1}(s) &= \left\{I + K_u^{-1}[(K_a+K_c)G_c + K_iG_i]\right\}^{-1}K_u^{-1}K_a \\ &= P\Big[K_uP + (K_a+K_c)Z_0^c + K_iZ_0^i\Big]^{-1}K_a \end{aligned} \tag{12}$$

The actuator disturbance response transfer function, T_{ur_1}, becomes

$$\begin{aligned} T_{ur_1}(s) &= -\left\{I + K_u^{-1}[(K_a+K_c)G_c + K_iG_i]\right\}^{-1}K_u^{-1}[(K_c+K_a)G_c \\ &\quad + K_iG_i] = -P\Big[K_uP + (K_a+K_c)Z_0^c + K_iZ_0^i\Big]^{-1} \\ &\quad \times \Big[(K_c+K_a)Z_0^c + K_iZ_0^i\Big]P^{-1} \end{aligned} \tag{13}$$

and finally the disturbance response transfer function, T_{yr_2}, becomes

$$\begin{aligned} T_{yr_2}(s) &= G_c\Big(I - \left\{I + K_u^{-1}\Big[(K_a+K_c)G_c + K_iG_i\Big]\right\}^{-1} \\ &\quad \times K_u^{-1}[(K_c+K_a)G_c + K_iG_i]\Big) = Z_0^c\Big\{I - \Big[K_uP + (K_a+K_c) \\ &\quad \times Z_0^c + K_iZ_0^i\Big]^{-1}\Big[(K_c+K_a)Z_0^c + K_iZ_0^i\Big]\Big\}P^{-1} \end{aligned} \tag{14}$$

B. Gain Matrix Structure

The controller structure introduced earlier is often used for aerospace applications and provides enough flexibility to design a closed-loop feedback system. The gains $K_a(s)$, $K_u(s)$, $K_c(s)$, and $K_i(s)$ are complex MIMO transfer functions that define the controller structure and need to be determined. For PEA, static and dynamic controllers are considered, unlike other eigenstructure assignment approaches. Tradeoffs between closed-loop properties can thus be performed, and this is made easier by having the closed-loop eigenspace as a design parameter. Although the controller structure and order can be adapted to satisfy additional and multiple criteria including stability, performance, decoupling, and robustness, in practice, the designer faces the difficult task of narrowing down the space of suitable controllers. In previous work [6,7], an alternative controller structure is introduced, where each gain function is a coprime factorization [14], which simplifies (8). Further decomposition of each matrix of the coprime factorization into singular value decomposition (SVD) and additional restrictions on the rotation matrices including static rotation matrices and some identical rotations led each gain matrix to take the form [8] $K(s) = L\Sigma_L(s)\Sigma_R(s)R$ where each component $\Sigma_i(s)$ is a diagonal rational polynomial diagonal matrix. After an initial placement of the controller poles and zeros, the tuning of gains and rotation matrices is investigated in a similar fashion to root locus for MIMO systems. Finally, additional metrics guide the choices and improve the performance, robustness, sensitivity, decoupling, and actuation dynamics.

In the work presented here, a systematic design tool is to be developed in the framework of LPV systems. The controller structure is chosen such that the controller gains are simply chosen as polynomial matrices which reduces the complexity of the search space for solutions and is better suited to the available tools for polynomial matrices. For the missile autopilot design, $K_a(s)$ is taken as a pure integrator, $\frac{I}{s}$, to ensure zero steady-state error for a steady demand. This in itself is usual in autopilot design, as the performance requirements, together with possible nonminimum phase zero transfer functions for acceleration control, can lead to slow or unstable designs.

C. Matching Conditions

When the system satisfies the Kimura condition [15], $n \leq r + m - 1$, where r is the number of inputs, m the number of outputs, and n the number of states, then pole placement for the whole closed-loop system can be performed. For the missile dynamics, this condition is met. Hence, full eigenstructure assignment is possible. For PEA this condition can be described by defining a desired closed-loop system and matching (11) to it. Such a

formulation can be written as a coprime factorization:

$$T_y^d(s) = N_d(s)D_d^{-1}(s) \tag{15}$$

where $D_d(s)$ is a polynomial matrix with the desired closed-loop eigenstructure and $N_d(s)$ is a polynomial matrix containing the open-loop zeros. By defining the desired closed-loop eigenstructure in this form, the effect of the system zeros can be managed in that they appear in the closed-loop transfer function. This implies that they are not canceled out by the controller structure, and the matching conditions (16) must hold. Hence, in the context of full feedback and with controller structure of Fig. 1, the feedback loop does not attempt to cancel open-loop zeros, but retains them by meeting Eq. (16a) by defining $N_d(s)$. As the controller has a free integrator, it has a steady-state closed-loop gain of one. Hence the determinants of $N_d(s)$ and $D_d s$ must be identical; this is reflected in condition (16b). Finally as the system has the same number of inputs as controlled outputs, matching $T_y(s)$ to $T_y^d(s)$ leads to (16c):

$$|N_d| = |Z_0^c| \tag{16a}$$

$$Z_0^c(0) = D_d(0) \tag{16b}$$

$$D_d(s)N_d^+(s) = \Big[sK_u(s)P(s) + sK_c(s)Z_0(s) + sK_i(s)Z_0^i(s) + Z_0^c(s)\Big]Z_0^{c+}(s) \tag{16c}$$

where the superscript + designates the polynomial adjoint matrix. The controller gains thus can be computed from (16c) by computing the left null space, which takes the form:

$$\begin{bmatrix} K_u(s) & K_c(s) & K_i(s) & I \end{bmatrix}\begin{bmatrix} P(s)Z_0^{c+}(s) \\ Z_0^c(s)Z_0^{c+}(s) \\ Z_0^i(s)Z_0^{c+}(s) \\ \frac{1}{s}\Big(Z_0^c(s)Z_0^{c+}(s) - D_d(s)N_d^+(s)\Big) \end{bmatrix} = 0 \tag{17}$$

This equation is used to select the controller which matches the desired closed-loop system. Note that if only partial feedback is available then the closed-loop transfer function is restricted, and not all closed-loop forms are attainable. This issue is dealt with in the paper when actuator dynamics are introduced.

The left polynomial null space is computed by simply reorganizing the polynomial matrices and applying a classic null space algorithm. This formulation enables the designed to specify the desired order for the controller by examining the effect of increasing the controller order on the ability to match the desired closed-loop structure. In fact, each polynomial matrix written in matrix polynomial form, $K(s)$,

$$K(s) = K_0 + K_1 s + K_2 s^2 + \cdots + K_n s^n \tag{18}$$

can be written in matrix coefficient form K:

$$K = \begin{bmatrix} K_n & \cdots & K_2 & K_1 & K_0 \end{bmatrix} \tag{19}$$

So Eq. (17) can be rewritten as

$$\begin{bmatrix} K_u(s) & K_c(s) & K_i(s) & I \end{bmatrix}\begin{bmatrix} PZ(s) \\ ZZ^c(s) \\ ZZ^{ic}(s) \\ ZZDN(s) \end{bmatrix} = 0 \tag{20}$$

Hence, solving for this null space with a first-order K_u and with constant matrices K_c, K_i, gives rise to a fourth-order closed-loop system and hence:

$$\begin{bmatrix} (K_u)_1 & (K_u)_0 & (K_c)_0 & (K_i)_0 & I \end{bmatrix}\begin{bmatrix} (PZ)_2 & (PZ)_1 & (PZ)_0 & 0 \\ 0 & (PZ)_2 & (PZ)_1 & (PZ)_0 \\ 0 & (ZZ^c)_2 & (ZZ^c)_1 & (ZZ^c)_0 \\ 0 & (ZZ^{ic})_2 & (ZZ^{ic})_1 & (ZZ^{ic})_0 \\ (ZZDN)_3 & (ZZDN)_2 & (ZZDN)_1 & (ZZDN)_0 \end{bmatrix} \tag{21}$$

where, for example, $(K_u)_i$ refers to the s^i coefficient matrix. For this system, the left null space of the right-hand matrix in (21) is calculated using a standard SVD algorithm, and takes the form:

$$\begin{bmatrix} X^{u_1} & X^{u_0} & X^{c_0} & X^{i_0} & X^{I_0} \end{bmatrix} \tag{22}$$

where $X^{\{u_{1,0},c_0,i_0,I_0\}}$ are constant matrices of appropriate column size, partitioned to match controller matrices column sizes. The number of rows of the null space in Eq. (22) determines whether a controller solution exists. If the row dimension of the null space is greater or equal to the number of system inputs, then a controller having the correct dimensions can be constructed from the null space. There is an extra condition that must be met for existence. This is that X^{I_0} must have full rank. This solution is then row reduced using Gaussian elimination to take the form:

$$\begin{bmatrix} Y_0^{u_1} & Y_0^{u_0} & Y_0^{c_0} & Y_0^{i_0} & I \\ Y_1^{u_1} & Y_1^{u_0} & Y_1^{c_0} & Y_1^{i_0} & 0 \end{bmatrix} \tag{23}$$

where $Y_{\{0,1\}}^{\{u_{1,0},c_0,i_0\}}$ are constant matrices of column size equal to their respective controller gains column sizes. The first row ensures the matching to the desired closed-loop system and if there are a sufficient number of rows in the second row, then a linear combination (in a polynomial sense) added to the first row will also satisfy the matching condition for the desired closed-loop system. If the controller space takes on this form, then additional criteria can be used to include performance, decoupling, and robustness by reference to the remaining transfer functions in Eq. (8).

D. LPV Approach to PEA

Eigenstructure assignment has many well-established numerical approaches to design and the main algorithms are surveyed in [13]. For linear parameter-varying systems, most approaches produce local controller designs that are interpolated over the operating envelope. The resulting controllers all suffer from gain scheduling problems associated with defining the controller, in particular, issues associated with zero and pole interpolation. More recently, work has been done on multimodel eigenstructure assignment that uses embedded models in the controller design and interpolation and

Table 1 Coefficients in nonlinear model (24)

	Interpolated formula
C_{y_v}	$0.5[(-25+M-60\|\sigma\|)(1+\cos 4\lambda)+(-26+1.5M-30\|\sigma\|)(1-\cos 4\lambda)]$
C_{y_ζ}	$10+0.5[(-1.6M+2\|\sigma\|)(1+\cos 4\lambda)+(-1.4M+1.5\|\sigma\|)(1-\cos 4\lambda)]$
C_{n_r}	$-500-30M+200\|\sigma\|$
C_{n_v}	$s_m C_{y_v}$, where $s_m = d^{-1}[1.3+0.1M+0.2(1+\cos 4\lambda)\|\sigma\|+0.3(1-\cos 4\lambda)\|\sigma\|-(1.3+m/500)]$
C_{n_ζ}	$s_f C_{y_\zeta}$, where $s_f = d^{-1}[2.6-(1.3+m/500)]$

which result in high order controllers. Model order reduction is then used to produce realistic controllers with promising results [16].

In this paper, the polynomial null space for PEA controllers is computed symbolically using the polynomial framework. The solution produces a generic controller and thus the usual gain scheduling problem is replaced by an explicit parameterization matching the parameterization of the LPV system itself. However, for the solution proposed in this paper, the PEA solution requires exact matching to the desired closed-loop system and thus the polynomial matrices $N_d(s,p)$ and $D_d(s,p)$ need to be chosen carefully. This condition will be relaxed in subsequent papers. The polynomial matrix $D_d(s,p)$ can be selected to be independent of the operating point p whereas polynomial matrix $N_d(s,p)$ is dependent on the open-loop zeros. The software package MATHEMATICA is used to form the polynomial null space and test for matching with the controller structure and order controlled throughout the operating envelope. The approach makes the closed-loop system independent of the current operating point and thus produces a solution similar to dynamic inversion without the need to consider zero dynamics.

III. Missile Lateral Autopilot Design

In this section polynomial eigenstructure assignment is applied to a quasilinear missile model, named the Horton missile model. The design leads to a linear parameter-varying controller for a side-slip velocity control. Although the underlying system is nonlinear, the closed-loop system is made independent of the operating points and can thus be compared to dynamic inversion approaches.

A. Missile Model

The Horton missile model describes a realistic airframe of a tail-controlled tactical missile in the cruciform fin configuration, as shown in Fig. 2. The aerodynamic parameters in this model are derived from wind-tunnel measurements [17,18]. The starting point for the mathematical description of the missile is the following nonlinear model [10,17,18] of the horizontal motion (on the xy plane in Fig. 2):

$$\begin{aligned}\dot{v} &= (M,\lambda,\sigma)v - Ur + y_\zeta(M,\lambda,\sigma)\zeta \\ &= \tfrac{1}{2}m^{-1}\rho V_0 S(C_{y_v}v + V_0 C_{y_\zeta}\zeta) - Ur \\ \dot{r} &= n_v(M,\lambda,\sigma)v + n_r(M,\lambda,\sigma)r + n_\zeta(M,\lambda,\sigma)\zeta \\ &= \tfrac{1}{2}I_z^{-1}\rho V_0 Sd\left(\tfrac{1}{2}dC_{n_r}r + C_{n_v}v + V_0 C_{n_\zeta}\zeta\right)\end{aligned} \tag{24}$$

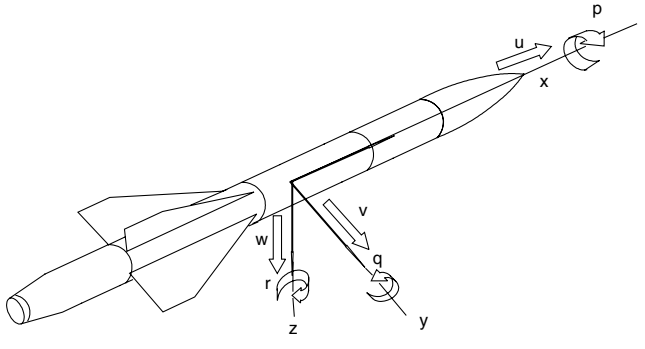

Fig. 2 Missile airframe axes.

where the variables are defined in Fig. 2. Here v is the side-slip velocity, r is the body rate, ζ the rudder fin deflections, y_v, y_ζ are semi-non-dimensional force derivatives due to lateral and fin angles, n_v, n_ζ, n_r are semi-non-dimensional moment derivatives due to side-slip velocity, fin angle, and body rate. Finally, U is the longitudinal velocity. Furthermore, $m = 125$ kg is the missile mass, $\rho = \rho_0 - 0.094h$ air density ($\rho_0 = 1.23\ \text{kg}\cdot\text{m}^{-3}$ is the sea level air density and h the missile altitude in km), V_0 the total velocity in $\text{m}\cdot\text{s}^{-1}$, $S = \pi d^2/4 = 0.0314\ \text{m}^2$ the reference area ($d = 0.2$ m is the reference diameter) and $I_z = 67.5\ \text{kg}\cdot\text{m}^2$ is the lateral inertia. For the coefficients C_{y_v}, C_{y_ζ}, C_{n_r}, C_{n_v}, and C_{n_ζ} only discrete data points are available, obtained from wind-tunnel experiments. Hence, an interpolation formula, involving the Mach number $M \in [2, 3.5]$, roll angle $\lambda \in [4.5\ \text{deg}, 45\ \text{deg}]$, and total incidence $\sigma \in [3\ \text{deg}, 17\ \text{deg}]$, has been calculated with the results summarized in Table 1.

The total velocity vector $\boldsymbol{V}_0$ is the sum of the longitudinal velocity vector $\boldsymbol{U}$ and the side-slip velocity vector $\boldsymbol{v}$, that is, $\boldsymbol{V}_0 = \boldsymbol{U} + \boldsymbol{v}$, with all three vectors lying on the xy plane; see Fig. 2. We assume that $U \gg v$, so that the total incidence σ, or the angle between $\boldsymbol{U}$ and $\boldsymbol{V}_0$, can be taken as $\sigma = v/V_0$, as $\sin\sigma \approx \sigma$ for small σ. Thus, we have $\sigma = v/V_0 = v/\sqrt{v^2+U^2}$, so that the total incidence is a nonlinear function of the side-slip velocity and longitudinal velocity, $\sigma = \sigma(v,U)$. As mentioned earlier the missile is in cruciform configuration; therefore symmetry assumptions are invoked. Hence despite the fact that the nonlinear model coefficients only depend on the absolute value of sigma, due to the symmetry assumptions the coefficients could be used for $v < 0$.

The Mach number is obviously defined as $M = V_0/a$, where a is the speed of sound, $a = 340 - 4h$. Since $V_0 = \sqrt{v^2+U^2}$, the Mach number is also a nonlinear function of the side-slip velocity and longitudinal velocity, $M = M(v,U)$.

It follows from the above discussion that all coefficients in Table 1 can be interpreted as nonlinear functions of three variables: side-slip velocity v, Mach number M, and roll angle λ.

B. Missile QLPV Form

Although the system in Eq. (24) is already in an QLPV form, theoretically one has to consider the linearization of the nonlinear system around its equilibria. For an equilibrium point (v_0, r_0, ζ_0) it is possible to derive from (24) models in incremental variables, $\delta v \doteq v - v_0$, $\delta r \doteq r - r_0$, and $\delta\zeta \doteq \zeta - \zeta_0$. In particular, for straight and level flight (with gravity influence neglected), we have $(v_0, r_0, \zeta_0) = (0,0,0)$, so that the incremental and absolute variables are numerically identical, although conceptually different. In the rest of this paper, the model defined in Eq. (25) can refer to the original QLPV form of the missile or its Taylor linearized version, as both forms present a QLPV form. Hence:

$$\begin{bmatrix}\delta\dot{v}\\ \delta\dot{r}\end{bmatrix} = \begin{bmatrix}y_v(p) & y_r(p)\\ n_v(p) & n_r(p)\end{bmatrix}\begin{bmatrix}\delta v\\ \delta r\end{bmatrix} + \begin{bmatrix}y_\zeta(p)\\ n_\zeta(p)\end{bmatrix}\delta\zeta \tag{25}$$

where p is the scheduling parameter.

Wind-tunnel tests are performed for the modeling of the missile but these experiments are usually conducted in some quasisteady conditions. This leads to an almost linearized version of the missile where the Mach number, roll angle, and incidence conditions have been included afterwards and which in the present case leads to a QLPV representation. Note that for a side-slip velocity controller, the

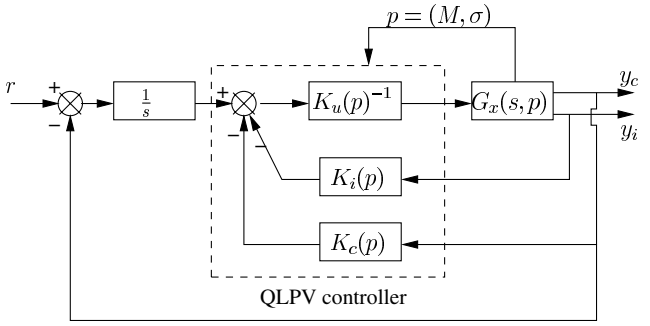

Fig. 3 The QLPV controller structure chosen for a lateral velocity controller of the Horton missile includes $K_a(s)$ as a pure integrator, $\frac{1}{s}$ and the gains $K_u(s)$, $K_c(s)$, $K_i(s)$ as scheduled scalar gains.

lateral acceleration demand is recast as a side-slip velocity demand via the nonlinear relationship $a = y_v(p)v + y_\zeta(p)\zeta$.

The controller structure presented earlier is now used in the LPV framework, as shown in Fig. 3, where gain $K_a(s)$ is selected as a pure integrator to ensure zero steady-state error to a step input. This form is shown to be sufficient to obtain a suitable controller with static controller gains. Note that, although the controller is presented in the figure as an LPV controller, the controller has a quasi-LPV static form.

C. Performance Objectives

In the context of the LPV system, polynomial eigenstructure assignment presented so far is strictly valid only for the underlying LTI system. However, one may assign the eigenstructure to be (almost) independent of the operating point. This would lead to (almost) identical closed-loop dynamics over the operating envelope. Being strictly independent is not always possible because the approach does not cancel out open-loop zeros and these may vary over the operating envelope. The resulting closed-loop dynamics, however, will be very similar to a LTI system dynamics, which is often desirable for the designer. Additional zeros may be included in the design to aid in placing the closed-loop system poles.

For static controller gains, the system is third order, that is, second-order plant and first-order pure integrator. The desired characteristic polynomial is of degree 3 and can be written as

$$D_d(s) = c_0 + c_1 s + c_2 s^2 + s^3 \tag{26}$$

Under the assumption that the zeros do not influence the response significantly, the closed-loop transient step response can be chosen to produce a peak overshoot less than 5% and settling time less than 0.2 s. The desired characteristic polynomial coefficients are thus chosen as a combination of a second order with natural frequency $w_n = 30$ rad/s and damping ratio $\zeta_n = 0.7$ and an additional pole at -100. The controller does not introduce additional zeros and there is no attempt to cancel out open-loop zeros, thus $N_d(s)$ is constrained by $Z_0^c(s)$ in condition (27a) and it represents the open-loop zeros.

The closed-loop transfer functions, in Eqs. (11) and (15) match the following LPV conditions:

$$N_d(s, p) = Z_0^c(s, p) \tag{27a}$$

$$Z_0^c(0, p) = D_d(0, p) \tag{27b}$$

$$\begin{aligned} D_d(s, p) = {} & [sK_u(s, p)P(s, p) + sK_c(s, p)Z_0(s, p) \\ & + sK_i(s, p)Z_0^i(s, p) + Z_0^c(s, p)] \end{aligned} \tag{27c}$$

where polynomial $D_d(s, p)$ and $N_d(s, p)$ represent the desired closed-loop transfer function. Note, it is not always possible to achieve exact matching or in other words to satisfy condition (27c) and a different controller structure and/or order may be required. However, for the SISO case presented here, this is straightforward and a static controller achieves matching.

Equation (27c) can be written as

$$\begin{bmatrix} K_u(s, p) & K_c(s, p) & K_i(s, p) & I \end{bmatrix} \begin{bmatrix} P(s, p) \\ Z_0^c(s, p) \\ Z_0^i(s, p) \\ \frac{1}{s}\left(Z_0^c(s, p) - D_d(s, p)\right) \end{bmatrix} = 0 \tag{28}$$

where the left null space solution is used to construct the controller gains. The null space has to be of sufficient dimension to allow reduction by Gaussian elimination to satisfy the annihilator vector format with the last term I. This is in fact equivalent to the condition in Eq. (27c). Finally, the null space solution may not be limited to a single solution and thus any "linear" (in the sense of polynomial) combination of row vectors that produces the annihilator vector format in Eq. (28) is suitable. From these null space solutions, the controller gains $K_u(s, p)$, $K_c(s, p)$, and $K_i(s, p)$ can be partitioned to produce a suitable controller for the controller structure shown in Fig. 3.

D. Side-Slip Velocity Controller

Consider a QLPV lateral velocity controller for the Horton missile for the case of state feedback. The output equation for side-slip velocity output is

$$\begin{bmatrix} y_c \\ y_i \end{bmatrix} = \begin{bmatrix} 1 & 0 \\ 0 & 1 \end{bmatrix} \begin{bmatrix} v \\ r \end{bmatrix} \tag{29}$$

This equation sets matrices $Z_0^c(s, p)$ and $Z_0^i(s, p)$, whereas $Z(s, p)$ and $P(s, p)$ are determined from the state equation. In fact, for this case, in Eqs. (4) and (29), $Z_0(s, p)$ is set equal to $Z(s, p)$, and the null space solution of Eq. (28) is then solved by symbolic computation using MATHEMATICA to yield the annihilator parameterized polynomial by p. After further row reduction the null space takes the vector form $[K_u\ K_c\ K_i\ I]^T$.

Equations (2) and (9) are computed and lead to $Z_0(s, p)$ and $P(s, p)$ which represent the coprime factorization of the system:

$$Z_0(s, p) = \begin{bmatrix} \frac{c_0(n_r(p)y_\zeta(p) - y_r(p)n_\zeta(p) - y_\zeta(p)s)}{n_r(p)y_\zeta(p) - y_r(p)n_\zeta(p)} \\ \frac{c_0(-n_v(p)y_\zeta(p) - y_v(p)n_\zeta(p) - n_\zeta(p)s)}{n_r(p)y_\zeta(p) - y_r(p)n_\zeta(p)} \end{bmatrix}$$

$$P(s, p) = \begin{bmatrix} \frac{c_0(y_r(p)n_v(p) - y_v(p)n_r(p) + y_v(p)s - n_r(p)s - s^2)}{n_r(p)y_\zeta(p) - y_r(p)n_\zeta(p)} \end{bmatrix} \tag{30}$$

The null space for Eq. (28) can now be solved as a polynomial equation, using the symbolic computation in MATHEMATICA. This produces a multivariable polynomial null space, the polynomial rank of which is 3 since the constituent vectors do not have any null elements and are independent. Any linear vector combination in this null space, provided it satisfies the constant last term I as in the vector $[K_u\ K_c\ K_i\ I]$ gives rise to a controller for the system.

The controller gains $K_u(s, p)$, $K_c(s, p)$, and $K_i(s, p)$ are identified by suitable partitioning of the resulting null space. For the present case, static controller gains are sufficient to obtain a matching condition for the desired closed loop and a unique LPV controller is obtained. The parameterized controller gains are as follows:

$$K_u = (n_\zeta y_r - n_r y_\zeta)\left[n_\zeta^2 y_r + n_\zeta(y_v - n_r)y_\zeta - n_v y_\zeta^2\right] \tag{31a}$$

$$\begin{aligned} K_c = {} & c_1 n_\zeta(n_\zeta y_r - n_r y_\zeta) + n_v(n_\zeta y_r - n_r y_\zeta)[n_\zeta y_r - (c_2 + n_r \\ & + y_v)y_\zeta] + n_\zeta\left[n_\zeta y_r y_v^2 - \left(c_0 + n_r y_v^2\right)y_\zeta + c_2 y_v(n_\zeta y_r - n_r y_\zeta)\right] \end{aligned} \tag{31b}$$

$$K_i = n_\zeta^2 y_r^2 y_v - c_1 n_\zeta y_r y_\zeta - 2n_r^2 n_\zeta y_r y_\zeta - n_v n_\zeta y_r^2 y_\zeta + c_0 y_\zeta^2 + n_r^3 y_\zeta^2 + c_2 (n_\zeta y_r - n_r y_\zeta)^2 + n_r \left[n_\zeta^2 y_r^2 - n_\zeta y_r y_v y_\zeta + (c_1 + n_v y_r) y_\zeta^2 \right] \tag{31c}$$

where parameterization in p is dropped for ease of presentation, and a common dividing factor given by Eq. (32) is omitted.

$$c_0 \left[n_\zeta^2 y_r + n_\zeta (y_v - n_r) y_\zeta - n_v y_\zeta^2 \right] \tag{32}$$

A direct substitution of the coefficients c_0, c_1, and c_2 of the desired closed-loop denominator of the system as well as of the QLPV semi-non-dimensional coefficients $y_v(p)$, $y_r(p)$, $y_\zeta(p)$, $n_v(p)$, $n_r(p)$, and $n_\zeta(p)$ leads to the desired controller (33).

$$\zeta = K_u(p)^{-1} \left(\frac{(v - v_d)}{s} - K_c(p) v - K_i(p) r \right) \tag{33}$$

E. Simulations

The controller developed in Sec. III.D is used in simulations with the QLPV Horton missile where parameter p includes both Mach number ranging in $[2, 3.5]$ and side-slip velocity, or implicitly incidence angle, ranging in $[-0.3, 0.3]$. The side-slip velocity demand is first prefiltered using a second-order filter ($\zeta = 0.7$, $w_n = 50$ rad/s). Two simulations are considered. First, a constant lateral acceleration demand of 100 $\mathrm{m \cdot s^{-2}}$ for a missile flying at a constant altitude of 6 km, with a Mach number varying linearly from Mach 2 to 3.5 in 3 s, as shown in Fig. 4. Notice that the side-slip velocity demand changes as the Mach number increases. This is due to a requirement for a constant lateral acceleration demand while dynamics of the missile system change over the flight envelope. This is achieved using the fact that there is a nonlinear relationship between side-slip velocity and lateral acceleration, given by $y_a = y_v(p) v + y_\zeta(p)$. Note moreover, that the dashed curves show the corresponding demands in lateral acceleration and side-slip velocity. The second simulation shows a change of lateral acceleration demand from -200 to 200 $\mathrm{m \cdot s^{-2}}$ at a Mach number of 2 for a missile flying at the altitude of 6 km and is shown in Fig. 5. Simulation responses for the nominal system show no steady-state error in side-slip velocity but some lag in the tracking of the side-slip velocity ramp (see Fig. 4). This is expected because only one pure integrator is present in the controller. The rise time criteria and peak overshoot criteria are satisfied, although the prefilter is responsible for part of the lag exhibited in the response. Note that the prefilter will eventually underestimate the peak overshoot because the prefilter is designed with a critical damping ratio. Hence the observed transient responses show that the autopilot meets all the design objectives set for side-slip velocity control.

IV. Polynomial Eigenstructure Assignment Including Actuator Dynamics

When actuators dynamics are included, an augmented system must be defined for the case of partial feedback, because the actuator states are usually not available for feedback. Hence, for this case, only partial eigenstructure assignment is possible for the augmented closed-loop system. So, Kimura's condition, $n \leq m + r - 1$ fails and therefore not all eigenvalues can be assigned independently.

In this section, the approach investigates the partial feedback case using the LPV framework, where both actuator requirements and/or system capabilities are investigated. The augmented system design should not include any actuator states for feedback leading to a system with partial feedback rather than state feedback. To explore the design issues, a full state solution is first computed and conditions on the feedback structure are imposed to remove the actuator states. Hence, the augmented system with full feedback is calculated initially. Then the actuator states feedback is removed which then results in a partial feedback solution. If the system design uses this approach it enables the designer to assess the effect of the actuator dynamics on the achievable eigenstructure. Hence tradeoffs between the speed of performance of the actuators and the overall system performance can be done. This is of importance as there is limited power and space available in missile structures, and the lowest actuator power solutions are strongly correlated with the actuator bandwidth. The effects of the actuator dynamics on the system's performance are studied by examining two different cases. First, the desired closed-loop system is selected and the actuator dynamics performance requirements are assessed. Secondly, specific actuator performance is selected and the achievable closed-loop system performance is determined. These are successively investigated in the case of lateral velocity, lateral augmented acceleration, and lateral acceleration controller designs for first- and second-order actuator dynamics models.

A. Matching Conditions with Full Feedback

For this case, the actuator states are feedback using a virtual output, y_l, and the controller structure is redefined including this virtual feedback with its corresponding virtual gain, $K_l(s, p)$

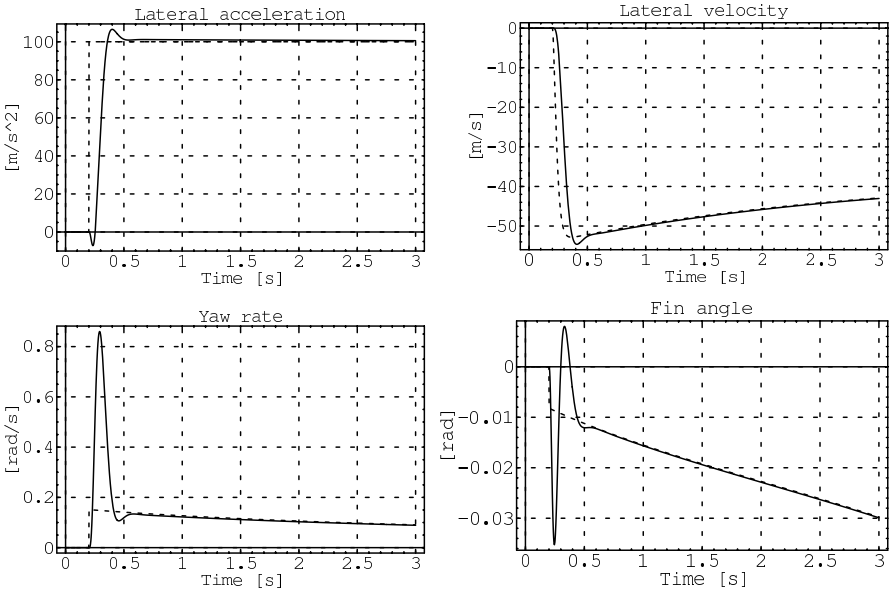

Fig. 4 Simulation of the Horton missile with side-slip velocity controller indirectly controlling a lateral acceleration demand of 100 $\mathrm{m \cdot s^{-2}}$ with Mach number varying linearly from Mach 2 to 3.5 in 3 s and constant altitude 6 km.

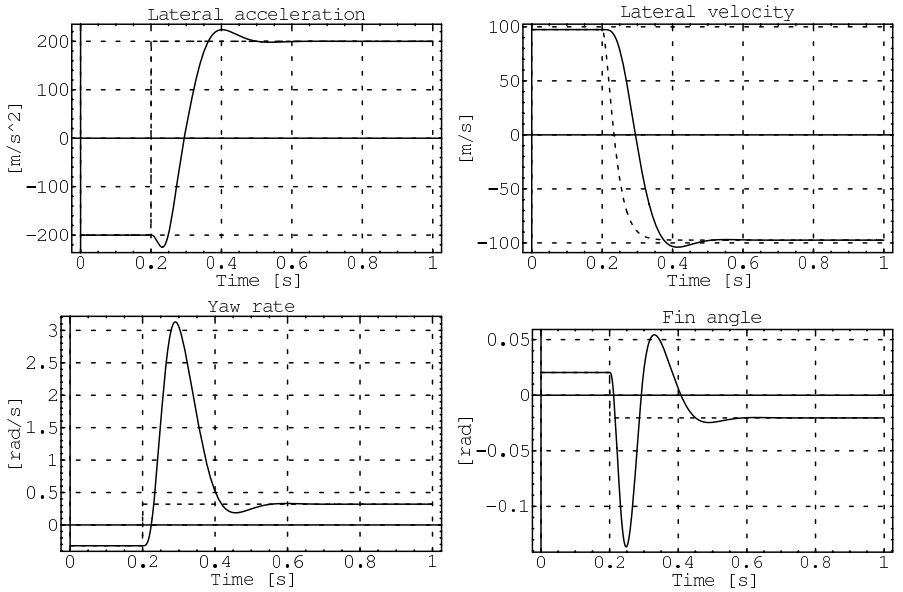

Fig. 5 Simulation of the Horton missile with side-slip velocity controller indirectly controlling a lateral acceleration demand changing from −200 to 200 m · s^{-2} at constant Mach number 2 and altitude 6 km.

(see Fig. 6). The controller is designed using polynomial eigenstructure assignment following Eq. (11), where $K_l(s, p)$ is obtained by suitable partitioning of $K_i(s, p)$. In a similar manner to the $G_i(s, p)$ transfer function, $G_l(s, p)$ and its associate $Z_0^l(s, p)$ can be introduced, which corresponds to the open-loop system between the inputs and the actuator states. The closed-loop transfer function can be derived from Eq. (11):

$$T_y(s,p) = Z_0^c(s,p)\Big[sK_u(s,p)P(s,p) + sK_c(s,p)Z_0^c(s,p) + sK_i(s,p)Z_0^i(s,p) + sK_l(s,p)Z_0^l(s,p) + Z_0^c(s,p)\Big]^{-1} \quad (34)$$

Splitting the overall transfer function into the corresponding controlled outputs transfer functions, measured outputs transfer function, and actuator states outputs transfer function does not affect the flexibility of the PEA approach. MIMO systems can also be dealt with in a similar manner without reducing controller gains to SISO or multiple input–single output (MISO) polynomial matrices.

However, conditions (27a–27c) still need to be satisfied as the desired closed-loop system is required to match the desired performance objectives. This is represented by conditions (35):

$$N_d(s,p) = Z_0^c(s,p) \quad (35a)$$

$$Z_0^c(0,p) = D_d(0,p) \quad (35b)$$

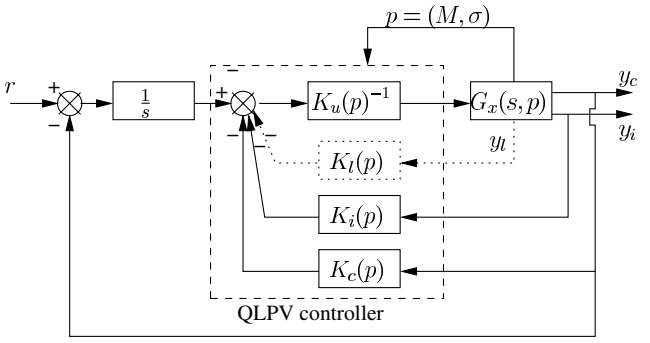

Fig. 6 The specific QLPV controller structure including actuator states feedback, y_l, through gain $K_l(s, p)$.

$$D_d(s,p) = \Big[sK_u(s,p)P(s,p) + sK_c(s,p)Z_0(s,p) + sK_i(s,p)Z_0^i(s,p) + sK_l(s,p)Z_0^l(s,p) + Z_0^c(s,p)\Big] \quad (35c)$$

where polynomial $D_d(s, p)$ and $N_d(s, p)$ represent the desired closed-loop transfer function. This can be written as a null space equation as

$$\begin{bmatrix} K_u(s,p) & K_c(s,p) & K_i(s,p) & K_l(s,p) & I \end{bmatrix} \times \begin{bmatrix} P(s,p) \\ Z_0^c(s,p) \\ Z_0^i(s,p) \\ Z_0^l(s,p) \\ \frac{1}{s}\Big[Z_0^c(s,p) - D_d(s,p)\Big] \end{bmatrix} = 0 \quad (36)$$

where the null space of this last vector gives direct access to the controller gains.

B. Lateral Acceleration Design with Full State Feedback Control

The full feedback design for a lateral acceleration controller performed on the augmented system including actuator dynamics is now considered. First-order actuator dynamics are assumed as follows:

$$\dot{l}(t) + \tau_l l(t) = \tau_l u(t) \quad (37)$$

where l represents the fin angle output from the actuator, u the command input, and τ_l the time constant of actuator dynamics.

The state equation for this augmented system becomes

$$\begin{bmatrix} \dot{v} \\ \dot{r} \\ \dot{l} \end{bmatrix} = \begin{bmatrix} y_v(p) & y_r(p) & y_\zeta(p) \\ n_v(p) & n_r(p) & n_\zeta(p) \\ 0 & 0 & -\tau_l \end{bmatrix} \begin{bmatrix} v \\ r \\ l \end{bmatrix} + \begin{bmatrix} 0 \\ 0 \\ \tau_l \end{bmatrix} u \quad (38)$$

and the output equation (39) includes the lateral acceleration and the yaw rate, together with the actuator state, fin angle l:

$$y = \begin{bmatrix} y_v(p) & 0 & y_\zeta(p) \\ 0 & 1 & 0 \\ 0 & 0 & 1 \end{bmatrix} \begin{bmatrix} v \\ r \\ l \end{bmatrix} + \begin{bmatrix} 0 \\ 0 \\ 0 \end{bmatrix} u \quad (39)$$

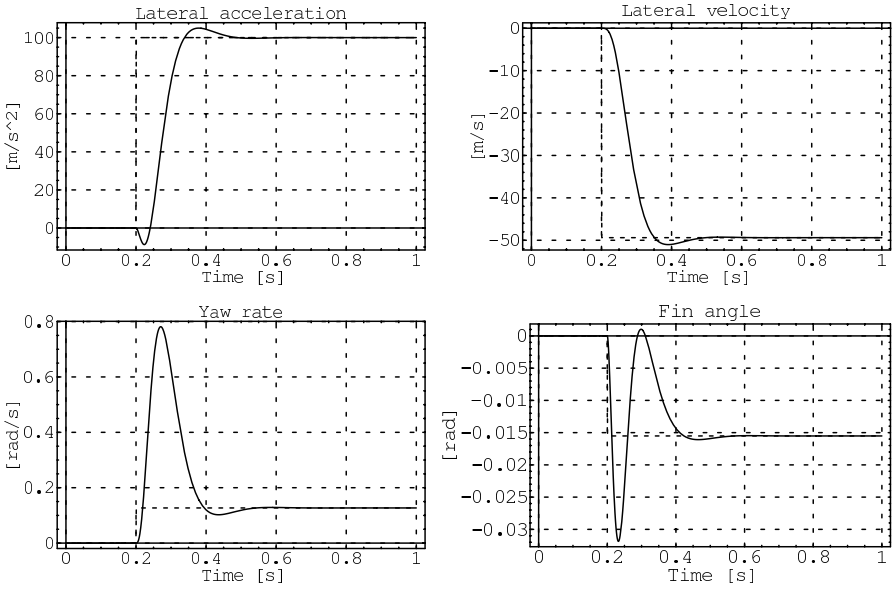

Fig. 7 Simulation of the Horton missile controlled in lateral acceleration and including actuator dynamics, in response to a lateral acceleration demand of 100 m · s^{-2} with constant Mach number 2.5 and constant altitude 6 km. The pole assignment of the closed-loop system is two poles at −60 and a conjugate pair with natural frequency 30 rad/s and critic damping ratio 0.7.

The D matrix normally present for lateral acceleration control vanishes due to the introduction of actuator dynamics; however, zeros are not affected and hence the nonminimum phase zero is still present.

In a similar manner to previous designs for this controllable and observable augmented system, a controller is derived by solving Eq. (36). The closed-loop system is shown to be fourth order due to the open-loop system being (second order) with actuator dynamics (first order) and an additional integrator in the control loop (first order) for steady-state accuracy. The full controller then takes the form:

$$u = K_u(s,p)^{-1}\left(\frac{(a-a_d)}{s} - K_c(s,p)a - K_i(s,p)r - K_l(s,p)l\right) \tag{40}$$

Simulations are carried out with actuator dynamics having a time constant $\tau_l = 300$. The four closed-loop system poles are chosen to be two poles at −60 and a conjugate pair with natural frequency 30 rad/s and critic damping ratio 0.7. Simulations for the Horton missile are shown in Fig. 7 and show satisfactory performance.

C. Lateral Acceleration Design with Partial State Feedback Control

In practice, the actuator states are not available and thus only partial feedback is possible. The idea is then to remove the virtual actuator feedback by zeroing the gain $K_l(s,p)$, thus constraining the achievable closed-loop system.

Preliminary studies using Nyquist plots using some reference actuator dynamics show that actuator dynamics is usually required to be 4–5 times faster than the desired closed-loop system. Although the studies presented in the paper confirm such results, the approach is more systematic and enables the designer to further analyze the closed-loop system performance as a function of actuator dynamics.

Hence, the full feedback design is amended by adding the requirement for the actuator feedback gain $K_l(s,p)$ to be zero. Doing so reduces the null space solution of Eq. (36) to a subset of its subspace and hence constrains either actuator dynamics or closed-loop system dynamics. Both cases are investigated.

After row reduction, the null space for Eq. (36) takes the form:

$$\begin{bmatrix} Y_0^{u_0} & Y_0^{c_0} & Y_0^{i_0} & Y_0^{l_0} & I \\ Y_1^{u_0} & Y_1^{c_0} & Y_1^{i_0} & Y_1^{l_0} & 0 \end{bmatrix} \tag{41}$$

where any linear combination (in the polynomial sense) of the second row added to the first row defines a possible controller. Specific linear combination are searched to identify the subspace which produces zero gain $K_l(s,p)$. However, this is not always possible and further conditions on either closed-loop structure or actuator dynamics can be imposed to generate suitable subspaces which contain zero gain solutions for $K_l(s,p)$. For instance, the rank of the polynomial space associated with $K_l(s,p)$ can be controlled by adding constraints on the closed-loop system pole assignment. This task is performed by symbolic computation using MATHEMATICA and thus a systematic design is achieved for some prespecified closed-loop eigenstructure assignment range. Such a null space takes the fundamental form:

$$\begin{bmatrix} Y_0^{u_0} & Y_0^{c_0} & Y_0^{i_0} & 0 & I \end{bmatrix} \tag{42}$$

with an alternative form given by

$$\begin{bmatrix} Y_0^{u_0} & Y_0^{c_0} & Y_0^{i_0} & 0 & I \\ Y_1^{u_0} & Y_1^{c_0} & Y_1^{i_0} & 0 & 0 \end{bmatrix} \tag{43}$$

where any linear combination (in the polynomial sense) of the second row added to the first row spans the space of suitable controllers.

Alternatively, when no suitable controller is found, the designer can choose either to increase controller order or to change controller structure. Increasing controller order may increase the null space and thus the space of suitable controllers. Changing the controller structure affects the design flexibility and eventually the matching capabilities.

D. Actuator Dynamics of First Order

Assuming actuator dynamics (37) of first-order augments the system by adding one state variable in a similar manner to Eq. (38). The output matrix as defined in (39) is slightly modified to define lateral augmented acceleration rather than pure lateral acceleration.

Equation (36) can then be solved in the form of (42) by imposing conditions on the actuator time constant τ_l while still achieving the desired closed-loop performance. The minimum actuator dynamics requirement in terms of time constant τ_l is shown in Fig. 8a for the lateral velocity and lateral augmented acceleration controller and in Fig. 8b for the lateral acceleration controller, for specific pole assignment of the overall closed-loop system. The pole assignment is chosen to be identical to the previous designs: two poles at −60 and a conjugate pair with natural frequency 30 rad/s and damping ratio

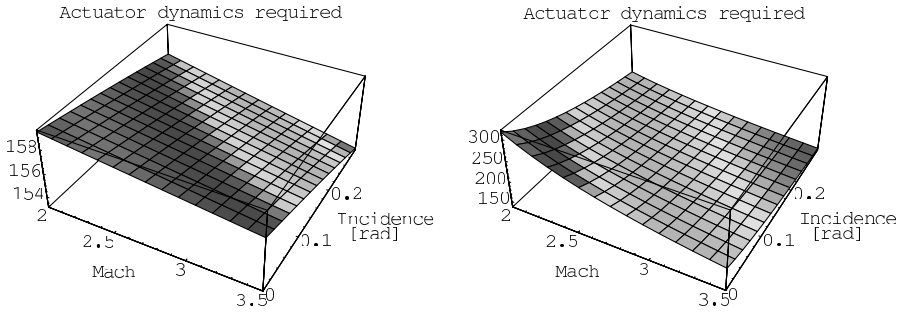

a) With lateral velocity or lateral augmented acceleration controller

b) With lateral normal acceleration controller

Fig. 8 Actuator dynamics time constant τ_l requirement for first-order actuator imposing the fourth-order closed loop with pole assignment: two poles at -60 and a conjugate pair with natural frequency 30 rad/s and damping ratio 0.7.

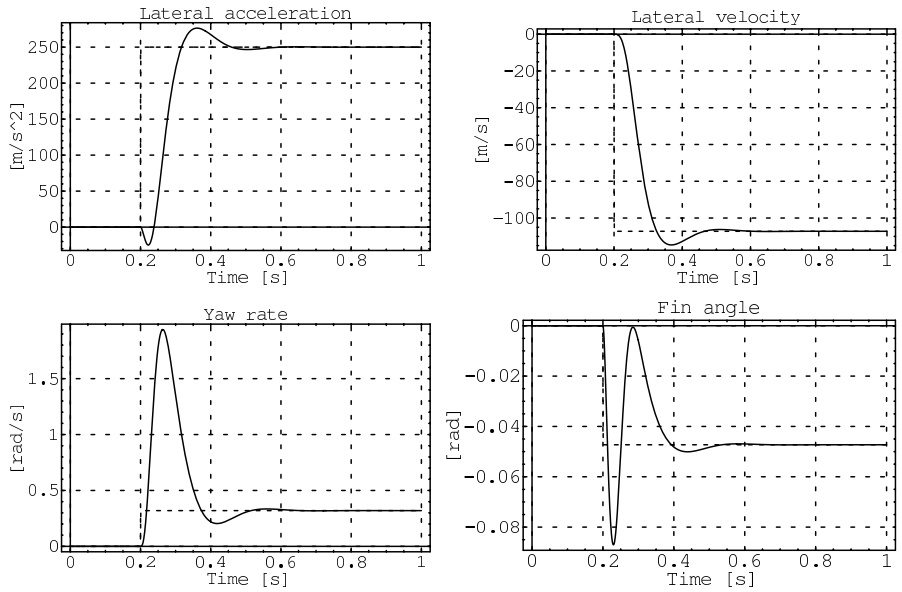

Fig. 9 Lateral acceleration step response of the Horton missile including first-order actuator dynamics with time constant, $\tau_l = 300$, for the lateral acceleration controller. The acceleration demand is 250 $\mathrm{m \cdot s^{-2}}$ while the Mach number is constant at 2.5 and altitude stays constant at 6 km.

0.7. The requirements for the lateral velocity design and lateral augmented acceleration design are identical; this is justified by the fact that they are simply related by the aerodynamic derivative $y_v(p)$. However, the lateral acceleration control results shown in Fig. 8b indicate that this is more demanding on actuator dynamics than the velocity controller. This is partly due to the fact that the nonminimum phase character of the controlled output has a significant part to play in the achievable performance.

Hence, the designer can characterize the actuator dynamics and can chose the maximum τ_l requirement across the flight envelope. For this case, a bandwidth of around 300 which corresponds to a cutoff frequency of around 50 Hz is a satisfactory solution. This choice ensures that the LPV system performs as required for a controller without actuator state feedback.

Next, the simulation for the lateral acceleration controller for a step input of 250 $\mathrm{m \cdot s^{-2}}$ is shown in Fig. 9

Once the actuator bandwidth has been chosen, it can be fixed. The performance across the flight envelope can be assessed by solving Eq. (34) while still maintaining $K_l(s, p) = 0$ while varying the closed poles of the system. Hence, the closed-loop system pole locations are not frozen across the flight envelope and this allows more flexibility in the design than for most dynamic inversion techniques.

In Fig. 10, pole locations vary slightly along the flight envelope where the first-order actuator dynamics is selected with time constant, $\tau_l = 300$. By design, the dominant conjugate pair is fixed with a natural frequency 30 rad/s and damping ratio 0.7 across the flight envelope, while the two other poles can vary but are always to the left of -60. In fact, selecting a more accurate upper bound for the time constant in the previous analysis would bring the worst case at exactly -60.

Finally, for a slow actuator system with a time constant $\tau_l = 150$, the closed-loop system cannot meet the pole location requirements and performance is affected (see Fig. 11). It can be seen that the

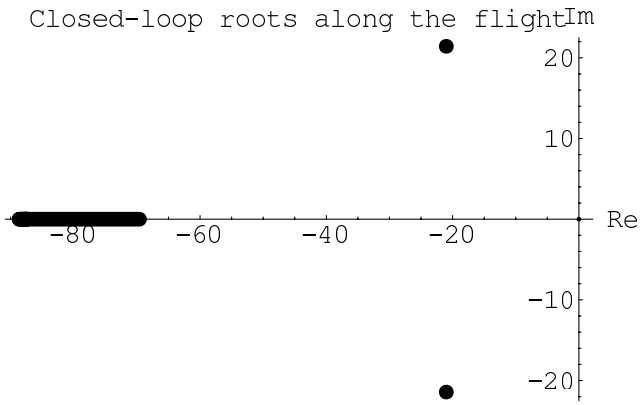

Fig. 10 Scenario of the poles location at Mach 2.5 across the flight envelope for the selected first-order actuator with time constant $\tau_l = 300$.

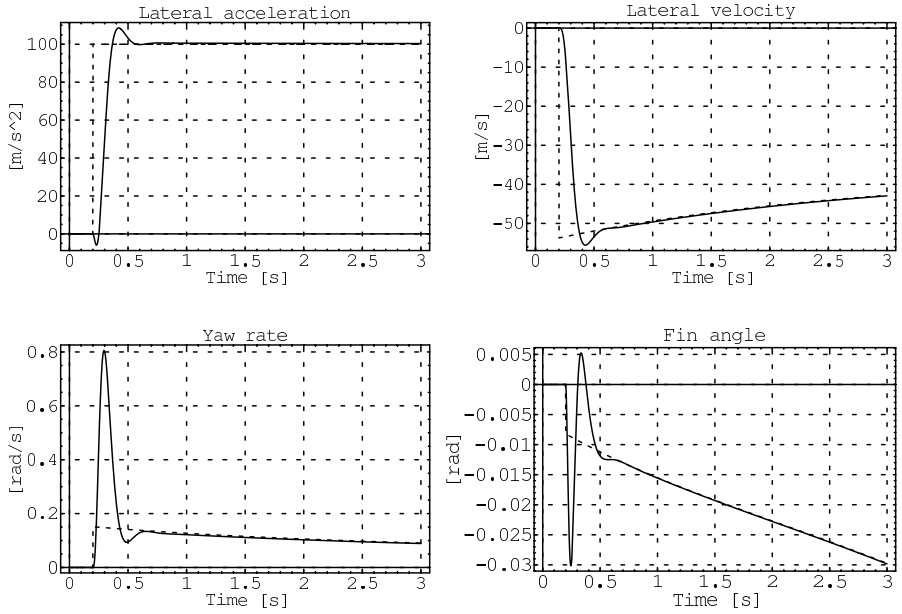

Fig. 11 Lateral acceleration step response of the Horton missile including an underspecified first-order actuator dynamics of time constant, $\tau_l = 150$, for the lateral acceleration controller. The acceleration demand is 100 m · s^{-2} while Mach number varies from Mach 2 to Mach 3.5 and altitude stays constant at 6 km.

actuator has less amplitude on Fig. 11 than Fig. 4, however, there is more acceleration overshoot.

E. Actuator Dynamics of Second Order

The same approach can apply to any actuator dynamics model order. For example, actuator dynamics of second order can be included and partial feedback solutions examined in a similar manner to the first-order actuator case. Actuator dynamics are then modeled as

$$\ddot{l} + 2\zeta_l \omega_l \dot{l} + \omega_l^2 l = \omega_l^2 u \tag{44}$$

where l represents the fin angle output, u the fin angle input, ω_l the natural frequency, and ζ_l the damping ratio of the actuator dynamics.

The system is now augmented by two state variables as

$$\begin{bmatrix} \dot{v} \\ \dot{r} \\ \dot{l}_1 \\ \dot{l}_2 \end{bmatrix} = \begin{bmatrix} y_v(p) & y_r(p) & y_\zeta(p) & 0 \\ n_v(p) & n_r(p) & n_\zeta(p) & 0 \\ 0 & 0 & 0 & 1 \\ 0 & 0 & -\omega_l^2 & -2\zeta_l\omega_l \end{bmatrix} \begin{bmatrix} v \\ r \\ l_1 \\ l_2 \end{bmatrix} + \begin{bmatrix} 0 \\ 0 \\ 0 \\ \omega_l^2 \end{bmatrix} u \tag{45}$$

and the output equation includes lateral acceleration, yaw rate along with fin angle and its first derivative, to give

$$y = \begin{bmatrix} y_v(p) & 0 & y_\zeta(p) & 0 \\ 0 & 1 & 0 & 0 \\ 0 & 0 & 1 & 0 \\ 0 & 0 & 0 & 1 \end{bmatrix} \begin{bmatrix} v \\ r \\ l_1 \\ l_2 \end{bmatrix} + \begin{bmatrix} 0 \\ 0 \\ 0 \\ 0 \end{bmatrix} u \tag{46}$$

The first row of the output matrix for lateral acceleration as defined in Eq. (46) is now changed for both lateral velocity or lateral augmented acceleration, but omitted here as it has similar structure.

With the same controller structure as previously defined, the null space Eq. (40) remains the same as for the first-order case, although $K_l(s, p)$ is now a vector of dimension two rather than one. Equation (36) is solved and results in the form of Eq. (42) by imposing conditions on the actuator dynamics, ω_l and ζ_l, while requiring the desired closed-loop performance to be achieved. The actuator dynamics requirements in terms of ω_l and ζ_l are presented in Fig. 12 for the lateral velocity and lateral augmented acceleration controller and in Fig. 13 for the lateral acceleration controller. The closed-loop system is now a fifth-order system with pole assignment similar to the previous first-order actuator study. Hence one pole is chosen at −60, with a conjugate pair with natural frequency 30 rad/s and damping ratio 0.7 and the other conjugate pair with natural frequency 110 rad/s and damping ratio 0.6. For the velocity and the lateral augmented acceleration controller case, the actuator dynamics requirements are around a natural frequency of 160 rad/s and a damping ratio in the range of 0.5–0.7. These requirements seem

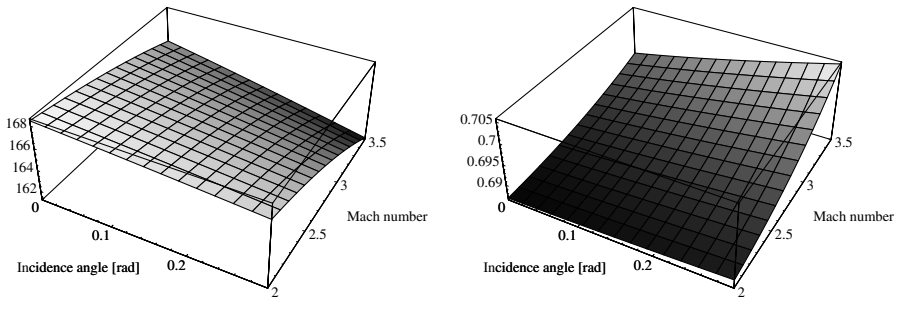

a) Natural frequency, ω_l **b) Damping ratio, ζ_l**

Fig. 12 For the lateral velocity or lateral augmented acceleration controller the actuator dynamics requirement on natural frequency ω_l and damping ratio ζ_l imposing the fifth-order closed loop with pole assignment: one pole at −60 and a conjugate pair at natural frequency 30 rad/s and damping ratio 0.7, and another conjugate pair at natural frequency 110 rad/s and damping ratio 0.6.

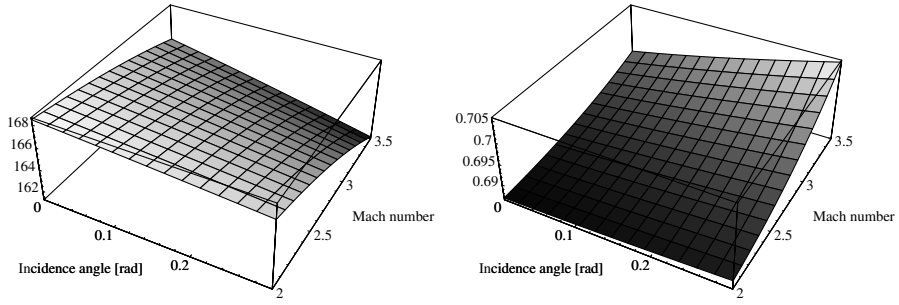

a) Natural frequency, ω_l **b) Damping ratio, ζ_l**

Fig. 13 For a lateral acceleration controller the actuator dynamics requirement on natural frequency ω_l and damping ratio ζ_l imposing the fifth-order closed loop with pole assignment: one pole at -60, a conjugate pair with natural frequency 30 rad/s and damping ratio 0.7, and a conjugate pair with natural frequency 110 rad/s and damping ratio 0.6.

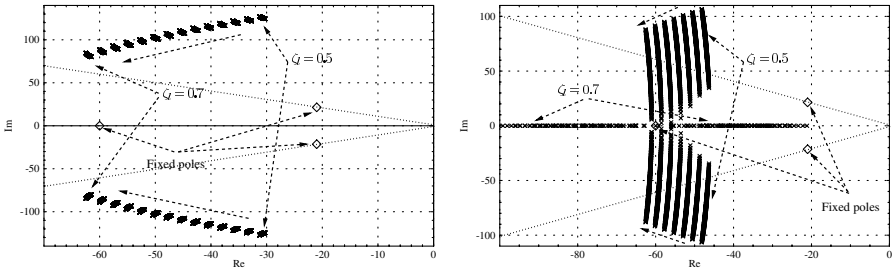

a) For lateral velocity or augmented acceleration control. **b) For lateral acceleration control**

Fig. 14 Scenario of the poles location across the flight envelope for a panel of second-order actuator with natural frequency 160 rad/s and damping ratio ranging from 0.5 to 0.7.

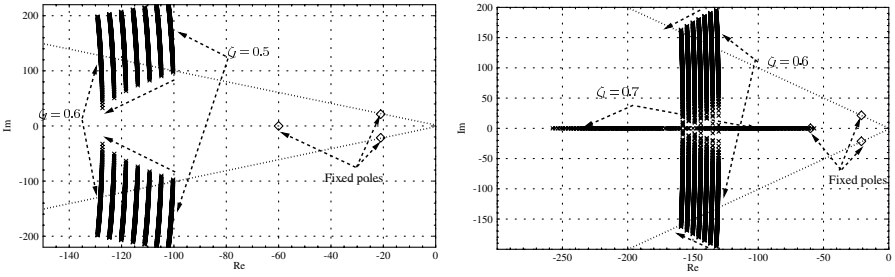

a) Damping ratio, ζ_l ranging from 0.5 to 0.6 **b) Damping ratio, ζ_l, ranging from 0.6 to 0.7**

Fig. 15 Scenario of the poles location across the flight envelope for a panel of second-order actuator with natural frequency 300 rad/s and varying damping ratio for lateral acceleration control.

reasonable because such actuator dynamics are practical. As already mentioned, the requirements for lateral velocity and lateral augmented acceleration are identical. As with the first-order actuator, the second-order actuator results have a more demanding requirement for actuator bandwidth due to the nonminimum phase character of the acceleration output. This is shown in Fig. 13, and a natural frequency of 240 rad/s for a damping ratio in a similar range of 0.5–0.7 is required to meet the closed-loop specifications.

In a similar manner to the first-order actuator dynamics case, once the actuator dynamics is fixed, the designer can assess the closed-loop system performance across the flight envelope by solving Eq. (34) while still maintaining $K_l(s) = 0$. The performance is estimated from the pole locations which change slightly along the flight envelope. The pole locations are found to be sensitive to the actuator damping ratio as shown in Fig. 14a where the actuator damping ratio sweeps from 0.5 to 0.7 while its natural frequency stays constant at 160 rad/s. By design, the dominant conjugate pair is frozen with a natural frequency 30 rad/s and damping ratio 0.7 with a pole fixed at -60 across the flight envelope. This results in the other conjugate pair varying significantly from slightly damped to underdamped. Selecting the same actuator dynamics for lateral acceleration control shows unsatisfactory pole locations in Fig. 14b. Selecting better actuator dynamics with higher frequency bandwidth as suggested by previous analysis leads to improved performance. For instance, the pole location for actuator dynamics with natural frequency around 300 rad/s and damping ratio ranging in $[0.5, 0.6]$ and $[0.6, 0.7]$ is shown in Figs. 15a and 15b, respectively.

V. Discussions and Conclusions

A successful lateral autopilot design is achieved for a realistic quasilinear parameter-varying missile model. This shows that QLPV models are amenable to dynamic inversion design of appropriate controllers using the same parameterization for plant and controller. The controller was obtained via polynomial eigenstructure assignment. The effects of the actuator bandwidth on the

closed-loop system performance were also studied, as was the requirement of dynamics and order of the actuators in order to achieve the desired performance.

The proposed QLPV controller is free of the difficulties associated with gain scheduling, as it consists of one controller only and "scheduling" is done automatically by feedback, giving total independence of the operating point. Nevertheless, the polynomial eigenstructure assignment design is only valid (as gain scheduling is) in the vicinity of the equilibria. The scheduling is directly performed with a QLPV controller and does not need any form of interpolation. The eigenvalues and eigenvectors of the resulting closed-loop system fully characterize its response and they are suitable to capture the control engineer objectives, stability, and performance. In essence, the approach achieves dynamic inversion, however, in contrast to the involved transformation does not require cancellation of the zero dynamics. It is consequently applicable to nonminimum phase systems as well and thus to a broader class, unlike other dynamic inversion approaches.

The PEA approach using the symbolic solutions enabled tradeoff studies to be undertaken that allow the designer to select the appropriate actuator bandwidth to produce a satisfactory performance. This is important in missile autopilots as there are usually limits placed on the power and energy available for the actuator.

References

[1] Blakelock, J. H., *Automatic Control of Aircraft and Missiles*, 2nd ed., Wiley, New York, 1991.

[2] Nielsen, J. N., *Missile Aerodynamics*, McGraw–Hill, New York, 1960.

[3] Roskam, J., *Airplane Flight Dynamics and Automatic Flight Controls*, Vol. 1, Roskam Aviation and Engineering Corporation, Ottawa, KS, 1979.

[4] Lin, C. F., *Modern Navigation, Guidance and Control Processing*, Prentice–Hall, Upper Saddle River, NJ, 1991.

[5] Siouris, G. M., *Airborne Missile Guidance and Control Systems*, Springer–Verlag, New York, 2003.

[6] White, B. A., "Flight Control of a VSTOL Aircraft Using Polynomial," *IEE UKACC, International Conference on Control 96*, Vol. 2, IEE, Sept. 1996, pp. 758–763.

[7] White, B. A., "Robust Polynomial Eigenstructure Assignment Using Dynamic Feedback Controllers," Proceedings of the Institution of Mechanical Engineers, Part 1, *Journal of Systems and Control Engineering*, Vol. 211, No. 1, 1997, pp. 35–51.

[8] White, B. A., "Robust Flight Control of a VSTOL Aircraft Using Polynomial Matching," *Proceedings of the American Control Conference*, American Automatic Control Council, Evanston, IL, June 1998, pp. 1133–1137.

[9] White, B. A., "Robust Control of an Unmanned Underwater Vehicle," *Proceedings of the 37th Conference on Decision & Control*, IEEE, Piscataway, NJ, Dec. 1998, pp. 2533–2534.

[10] Horton, M. P., "A Study of Autopilots for the Adaptive Control of Tactical Guided Missiles," M.S. Thesis, University of Bath, 1992.

[11] Liu, G. P., and Patton, R. J., *Eigenstructure Assignment for Control System Design*, Wiley, Chichester, 1998.

[12] Söylemez, M. T., *Pole Assignment for Uncertain Systems*, UMIST Control Systems Center Series, Research Studies Press, Baldock, 1999.

[13] White, B. A., "Eigenstructure Assignment: A Survey," Proceedings of the Institution of Mechanical Engineers, Part 1, *Journal of Systems and Control Engineering*, Vol. 209, No. I1, 1995, pp. 1–11.

[14] Kailath, T., *Linear Systems*, Prentice–Hall, Upper Saddle River, NJ, 1980.

[15] Kimura, H., "Pole Assignment by Gain Output Feedback," *IEEE Transactions on Automatic Control*, Vol. 20, No. 4, Aug. 1975, pp. 509–516.

[16] Magni, J.-F., *Robust Modal Control with a Toolbox for Use with Matlab*, Kluwer Academic/Plenum, New York, 2002.

[17] Tsourdos, A., Żbikowski, R., and White, B. A., "Robust Design of Sideslip Velocity Autopilot for a Quasi-Linear Parameter-Varying Missile Model," *Journal of Guidance, Control, and Dynamics*, Vol. 24, No. 2, 2001, pp. 287–295.

[18] Bruyère, L., Tsourdos, A., Żbikowski, R., and White, B. A., "Robust Performance Study for Lateral Autopilot of a Quasi-Linear Parameter-Varying Missile," *Proceedings of the 2002 American Control Conference*, American Automatic Control Council, Evanston, IL, Vol. 1, 2002, pp. 226–231.